

RSC Advances



This is an *Accepted Manuscript*, which has been through the Royal Society of Chemistry peer review process and has been accepted for publication.

Accepted Manuscripts are published online shortly after acceptance, before technical editing, formatting and proof reading. Using this free service, authors can make their results available to the community, in citable form, before we publish the edited article. This *Accepted Manuscript* will be replaced by the edited, formatted and paginated article as soon as this is available.

You can find more information about *Accepted Manuscripts* in the [Information for Authors](#).

Please note that technical editing may introduce minor changes to the text and/or graphics, which may alter content. The journal's standard [Terms & Conditions](#) and the [Ethical guidelines](#) still apply. In no event shall the Royal Society of Chemistry be held responsible for any errors or omissions in this *Accepted Manuscript* or any consequences arising from the use of any information it contains.

Fluorescent single walled carbon nanotube-mediated sensors with detection limit of $\sim 10^{-8}$ M for nitrophenol based chemical warfare agents and environmental pollutants.



341x146mm (150 x 150 DPI)

Sensing Properties of Light-Emitting Single Walled Carbon Nanotubes Prepared via Click Chemistry of Ylides Bound to Nanotube Surface

Cite this: DOI: 10.1039/x0xx00000x

M.K. Bayazit,^{*a,b} L.O. Pålsson^a and K.S. Coleman^a

Received 00th January 2012,

Accepted 00th January 2012

DOI: 10.1039/x0xx00000x

www.rsc.org/

Pyridinium ylide functionalized single-walled carbon nanotubes (SWCNTs) generated from simple quaternary pyridinium salts covalently bound to SWCNT surface undergo a 1,3 dipolar cycloaddition with dimethyl acetylenedicarboxylate in a 'click' chemistry type fashion to yield indolizine modified light-emitting SWCNTs. Conversion of quaternary pyridinium salts into indolizines on SWCNT surface was confirmed by XPS, fluorescence spectroscopy and optical microscopy. The resulting modified SWCNTs were found to emit blue light when excited at 330 nm. Fluorescent quenching experiments performed via nitroaromatic compounds displayed that the fluorescence of modified SWCNTs quenched by nitrophenol derivatives in both solution-state and solid-state, probably due to strong H-bonding interaction between host and guest molecule. Functionalized SWCNTs were further characterized using TGA-MS, FTIR and UV-vis-NIR spectroscopy.

Introduction

Chemical sensing has gained much attention due to increasing demand for monitoring environmental pollution, detecting warfare and security threats, developing diagnostics for medical care and providing efficient and sensitive tools for quality control in industrial applications¹. Due to their interesting chemical and physical properties carbon nanotubes (CNTs) have been used for chemical sensor applications, each based on alterations in a particular feature of functional material including conductivity for chemiresistors^{2, 3} and back gate field effect transistors³⁻⁶ and intensity of scattered light resulted by the adsorption of chemical species for photo chemical or optical sensors⁷⁻¹¹. Substantial effort, therefore, has been devoted in fabricating SWCNT based sensors and the surface functionalization of CNTs in order for utilizing them for sensing. Following the discovery of bright fluorescence in the 800- to 1600 nm wavelength range of the near infrared from one-dimensional direct band gap semiconducting tubes,¹² a SWCNT based near-infrared optical sensor for glucose detection was fabricated by assembling a monolayer of the enzyme on nanotube surface followed by ferricyanide functionalisation.¹³ Pyrene-modified β -cyclodextrin-decorated SWCNT field-effect transistor device as a photosensor was used to probe a fluorescent adamantyl-modified Ru complex through a charge-transfer mechanism from pyrenecyclodextrin-SWCNT hybrids to adamantyl-modified Ru complex.¹⁴ A chemiresistive sensor based on SWCNT and hexafluoroisopropanol functionalised polythiophene for the detection of chemical warfare agents including sarin gas and dimethyl methylphosphonate has been shown by a simple spin-casting technique,³ where the sensory response was investigated measuring the conductance of the SWCNT deposition. Fabrication of fluorescent chemosensors were achieved by covalently quinoline modified CNTs for Cu²⁺ and Zn²⁺ ions^{15, 16} and CNTs bearing adsorbed DNA with 6-carboxyfluorescein groups for Hg²⁺.¹⁷

Introducing surface groups also enhanced the processability of CNTs, particularly SWCNTs, in both aqueous and non-aqueous solvents by interrupting the strong van der Waals forces causing aggregation or bundling of the material. Covalent strategies to functionalize SWCNTs have included carbene,¹⁸ radical,^{19, 20} cycloaddition,²¹⁻²⁴ organolithium addition^{25, 26} and oxidation^{27, 28}

reactions and been recently reviewed.²⁹ Among radical reactions aryl diazonium salts addition^{19, 30-34} has widely been studied using diazonium salts directly³⁰ or generating them in-situ by oxidation of the corresponding aniline with inorganic³¹ or organic³² oxidants. In our research group, it was shown that pyridine diazonium salts underwent a radical addition reaction to SWCNTs to yield pyridine-functionalized SWCNTs which were able to act as cross-linkers and hydrogen bond to poly(acrylic acid) to form SWCNT hydrogels.³⁵ 'Click' chemistry, defined as a modular reaction bringing together two simple units to generate a more complex substance, is gaining momentum in materials science.^{21, 36} For CNTs 'click' chemistry is predominately based around the Huisgen cycloaddition of azides to alkynes and has been used to attach polystyrene,³⁷ β -cyclodextrin³⁸ and phthalocyanines³⁹ to the surface of nanotubes. Although other simple 1,3-dipolar cycloaddition reactions also fit the criteria of 'click' chemistry such as the reaction described here.

Herein diazonium salt addition and 1,3-dipolar cycloaddition reactions were utilized in a modular type fashion to introduce light emitting groups to the surface of SWCNTs in a 'click' chemistry type fashion at low temperatures. Fluorescent SWCNTs were tested as sensor to probe nitroaromatic compounds in both solution-state and solid-state.

Experimental

Material Preparation. 1. SWCNTs. Purified SWCNTs, produced by the HiPco method, were purchased from Unidym, USA, and further purified by heating in air at 400 °C and soaking in 6M HCl overnight. The purified SWCNTs were isolated by filtration over a polycarbonate membrane (0.2 μ m, Whatman), and washed with copious amounts of high-purity water until pH neutral. The purified SWCNTs were annealed under vacuum (10⁻² mbar) at 900°C to remove residual oxygen containing functional groups and any adsorbed gases or solvents.

2. SWCNT-Pyridine (SWCNT-Py). SWCNT-Py was prepared following the literature procedure.³⁵ In brief, pyridine diazonium salt generated was reacted with SWCNTs at 0 °C in *N,N*-dimethylformamide (DMF). The modified SWCNTs were filtered

through a nylon membrane (0.2 μm , Whatman), re-dispersed in 2 M HCl (100 mL), filtered and washed with copious amount of water until pH neutral. The resulting solid material was dispersed in 2 M NaOH (100 mL) and stirred overnight to ensure deprotonation of the pyridinium salt to pyridine. The functionalized SWCNTs were then isolated by filtration through a nylon membrane (0.2 μm , Whatman) and washed with water until pH neutral and re-dispersed and filtered using THF (2 \times 30 mL), acetone (2 \times 30 mL) and ethanol (2 \times 30 mL), respectively and dried overnight at 80 $^{\circ}\text{C}$ to afford SWCNT-Py.

3. SWCNT-Pyridinium Ester Salt (1a). To a dispersion of SWCNT-Py (5 mg) in dry DMF (10 mL), dispersed using an ultrasonic bath (Ultrawave U50, 30 – 40 kHz) for 5 mins, was added ethyl-2-bromoacetate (5 mL, 7.53 g, 45.09 mmol) and the reaction mixture stirred at room temperature for 12 hours. The SWCNTs were then filtered through a nylon membrane (0.2 μm , Whatman), re-dispersed in acetone (30 mL), filtered and washed with acetone (2 \times 30 mL) and dried overnight at 80 $^{\circ}\text{C}$ to afford SWCNT-pyridinium ester (**1a**).

Results and discussion

Herein, an elegant synthetic protocol to introduce light-emitting groups to the surface of SWCNTs via diazonium salt addition followed by 'click' chemistry is demonstrated using the reactivity of pyridine lone pair. The pyridinium ylide, rather than reacting with the CNT surface directly, is covalently bonded to the nanotube which then undergoes 1,3-dipolar cycloaddition with dimethyl acetylenedicarboxylate (DMAD) to yield fluorescent indolizines, **Scheme 1**. In contrast to previously reported method,^{21, 23} combined diazonium salt-click chemistry approach described here offers high yielding indolizine formations at low temperatures, more control on reaction conditions, possible choice of dipoles/dipolarophiles with desired side groups (e.g. cyclodextrins,⁴⁰ activated alkynes or alkenes at low temperatures⁴¹) and the characterization of reaction intermediates. It may further provide a route to generate various quaternary pyridinium salts bearing alkyl, aryl or polymers (e.g. poly(ethylene glycol)) that is likely to enhance the solubility and processability of SWCNT material. However, multistep surface functionalization of SWCNTs resulted in low yields of isolated products that had noteworthy effect on the characterization of modified SWCNTs by concentration/thickness dependent techniques including FTIR and XPS.

In agreement with the previous literature findings,³⁵ electronic spectrum of SWCNT-Py in DMF showed suppressed van Hove singularities, indicative of covalent surface modification. (see *ESI Figure S1*) A stable dispersion of SWCNT-Py had a concentration of $\sim 160 \mu\text{g mL}^{-1}$, calculated using the Beer's law and an extinction coefficient of $30 \text{ mL mg}^{-1} \text{ cm}^{-1}$ and absorption values at $\lambda = 700 \text{ nm}$,⁴² which decreased dramatically to $0.2 \mu\text{g mL}^{-1}$ upon the addition of ethyl-2-bromoacetate to form the Kröhnke salt (**1a**) which increased to $40 \mu\text{g mL}^{-1}$ following 'click' reaction to form the indolizine functionalized SWCNTs (**1b**). Table 1 shows the solubility of the stable dispersion of Kröhnke salt modified SWCNTs (**1a**, **2a** and **3a**), indolizine functionalized SWCNTs (**1b**, **2b** and **3b**) and pyridine functionalized SWCNTs (SWCNT-Py) in both DMF and ethanol (EtOH). Solubility of SWCNT-Py in both DMF and EtOH decreased after the formation of **1a**, **2a** and **3a**. However, solubility in DMF increased after the cycloaddition reaction to yield indolizines while the solubility of in EtOH decreased, probably due to solute/solvent interactions.

Table 1. Solubility data ($\mu\text{g/mL}$) of 1a-3a, 1b-3b and SWCNT-Py in both DMF and EtOH.

	SWCNT-Py	1a	2a	3a	1b	2b	3b
DMF	160	0.2	8.4	3.9	40.0	47.4	10.1
EtOH	72.4	34.0	28.5	3.1	16.4	19.3	1.26

The ATR-FTIR spectra of **1b-3b**, **Figure 1**, displayed the presence of the ester groups attached to the indolizine ring as a broad band ($\nu_{\text{C=O}}$) centred around 1730 cm^{-1} (along with multiple bands between $1600\text{-}1300 \text{ cm}^{-1}$, presumably from the formation of the indolizine).⁴³ The bands *ca.* $2850\text{-}2990 \text{ cm}^{-1}$ in the spectrum of **3b** that are up-shifted compared with **1b** were attributed to the aromatic C-H stretching, and the band at 1270 cm^{-1} indicated the $-\text{NO}_2$ symmetric stretching (ν_{NO_2} 1270 cm^{-1}), confirming the presence of nitro groups.^{44,45} The FTIR spectrum of **2b** was noisy compared to others, probably due to the thickness of the film prepared.

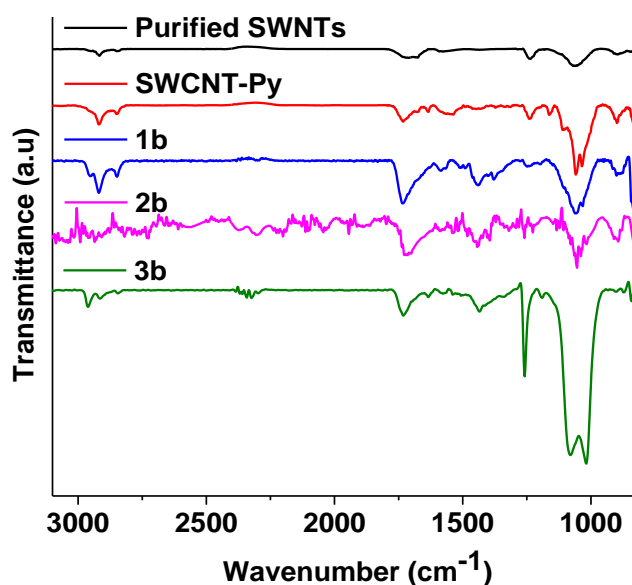


Figure 1. Normalized and offset ATR-FTIR spectra of purified SWCNTs (black line), SWCNT-Py (red line), **1b** (blue line), **2b** (magenta line) and **3b** (olive line). All spectra were recorded using SWCNT films. Curves in are in top-down, respectively.

TGA of **1b**, **2b** and **3b** showed a weight loss of ~ 38 , 35 and 64% respectively, at $600 \text{ }^{\circ}\text{C}$ compared to *ca.* 7% for purified SWCNTs (**Figure 2**). Weight losses of **1b**, **2b** and **3b** correspond to the presence of approximately 1 indolizine group for every 56 ($1.77 \text{ N}\%$), 76 ($1.32 \text{ N}\%$) and 142 ($0.70 \text{ N}\%$) nanotube carbon atoms, respectively, assuming the whole weight loss is due to removal of surface indolizines. Mass spectrometry results revealed that the indolizine groups were covalently attached to nanotube surface, showing common fragments at high temperatures for the indolizine modified SWCNTs (**Figure 3**). The mass fragments detected by mass spectrometry demonstrated that **1b** fragmented into methyl ester group (*OMe*, 31 amu), ethyl ester group (*OEt*, 45 amu) and *N*-methylpyridinium ($\text{C}_6\text{H}_8\text{N}$, 94 amu) *ca.* $300\text{-}500 \text{ }^{\circ}\text{C}$, although the parent ion of the indolizine was not observed.

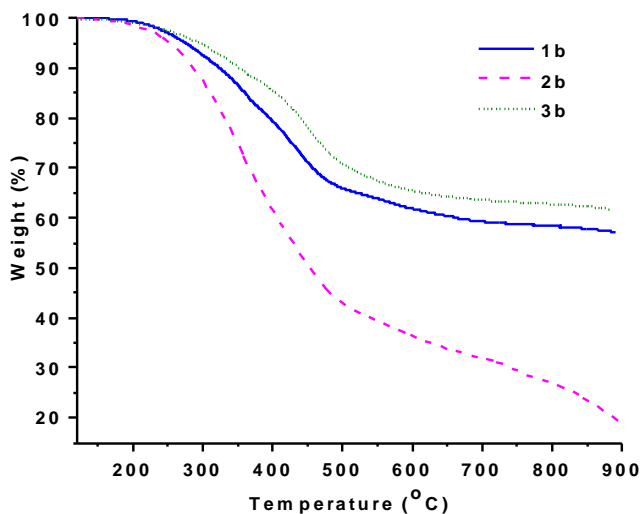
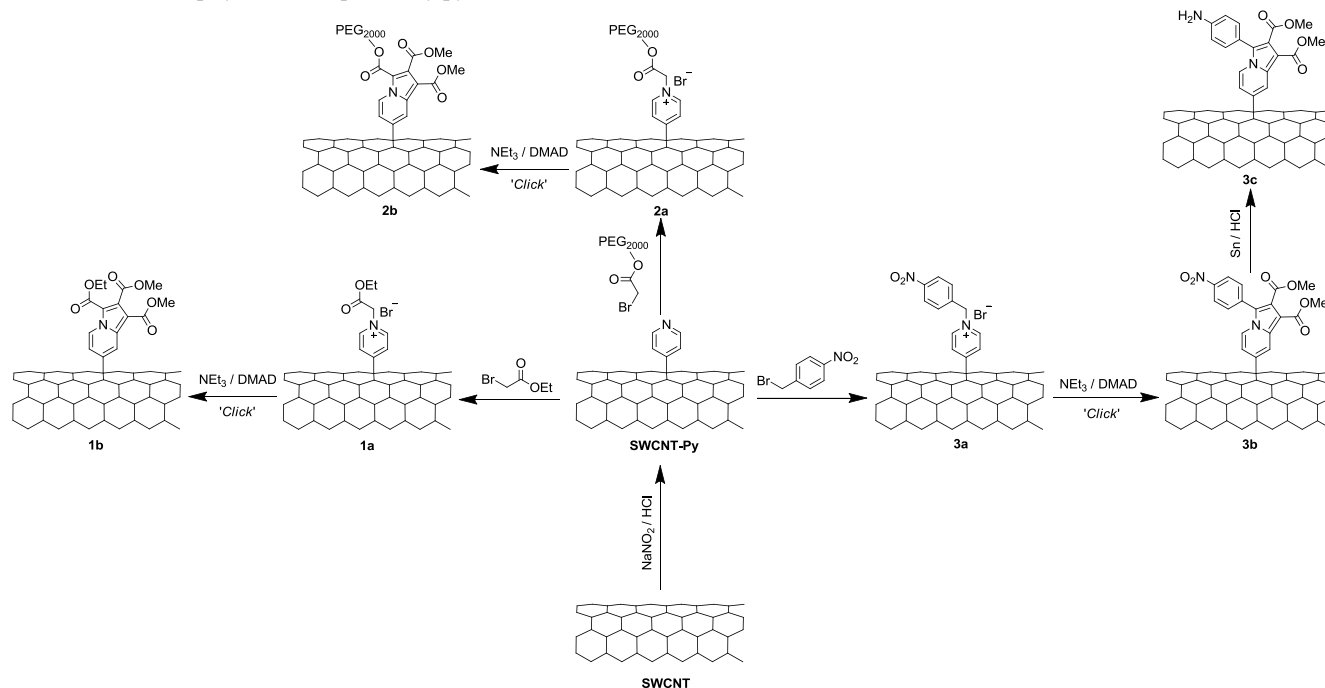
Scheme 1. Multistep synthesis of quaternary pyridinium salt and indolizine modified SWCNTs (**1a-3a**, **1b-3b** and **3c**).

Figure 2. TGA data of **1b** (blue line), **2b** (magenta dashed line) and **3b** (green dotted line). Data were recorded in flowing He (20 mL min⁻¹) at a ramp rate of 10 °C min⁻¹ to 900 °C after being held at 120 °C for 30 mins to remove any residual solvent.

Mass spectrometry data recorded for the poly(ethylene glycol) containing indolizine modified SWCNTs (**2b**) displayed the presence of methyl ester (*OMe*, 31 amu), *N*-methylpyridinium (*C₆H₈N*, 94 amu) and ethyl formyl group (*OCOCH₂CH₃*, 73 amu) as an indicative of the poly(ethylene glycol) grafted indolizine modified SWCNTs. Fragmented methyl ester group (*OMe*, 31 amu), *N*-methylpyridinium (*C₆H₈N*, 94 amu), phenyl group (*C₆H₄*, 76 amu),

nitroso group (*NO*, 30 amu) and phenoxy group (*C₆H₄O*, 93 amu) confirmed the presence of a nitro phenyl group attached on **3b**.

In order to confirm the pyridinium salt formation and their conversion into indolizine via 'click' reaction, quaternary pyridinium salt modified (**1a** and **3a**) and indolizine modified (**1b** and **3b**) SWCNTs were further analyzed by X-ray photoelectron spectroscopy (XPS). **Figure 4** shows deconvoluted N 1s XPS spectra of (**1a**, **1b**, **3a** and **3b**). The deconvoluted N 1s XPS spectrum of **1a** showed three peaks that can be probably attributed to the quaternary nitrogen (*N⁺*) at ca. 402.3 eV,^{23, 46} pyridinic nitrogen at 398.9 eV^{21, 23, 35} and pyridine radical cation (*N^{•+}*) at 400.2 eV.^{47, 48} After the 'click' reaction of **1a** with DMAD, the deconvoluted N 1s XPS spectrum of **1b** displayed two unchanged peaks positioned at ca. 399.9 and 398.9 eV and a new peak generated at 401.4 eV that probably correspond to indolizine ring nitrogen (*-N<*).⁴⁹ The deconvoluted N 1s XPS spectrum of **3a** showed signature of nitro group (*-NO₂*),²³ pyridine diazo (*-N=N*),⁵⁰ quaternary nitrogen (*N⁺*)²³ and pyridine radical cation (*N^{•+}*)^{47, 48} at ca. 406.2, 403.8, 402.4 and 400.1, respectively. Similar to **1b**, after the 'click' reaction, the deconvoluted N 1s XPS spectrum of **3b** displayed a new peak formation positioned at ca. 401.5 eV as an indication of indolizine formation. N 1s XPS spectra of both **1b** and **3b** showed no peak related to quaternary pyridinium nitrogen (*N⁺*), confirming that pyridinium salts were successfully converted into pyridinium ylides, which subsequently reacted with DMAD to yield indolizines. Compared to the atomic per cent (at.%) nitrogen (2.90 %) found in SWCNT-Py, XPS elemental analysis results of **1b**, **2b** and **3b** verified the presence of 2.22±0.33, 1.60±0.22 and 2.16±0.56 atomic per cent (at.%) nitrogen, respectively, suggesting nitrogen free new group addition (e.g. DMAD, PEG, benzene ring etc.) to SWCNT surface.

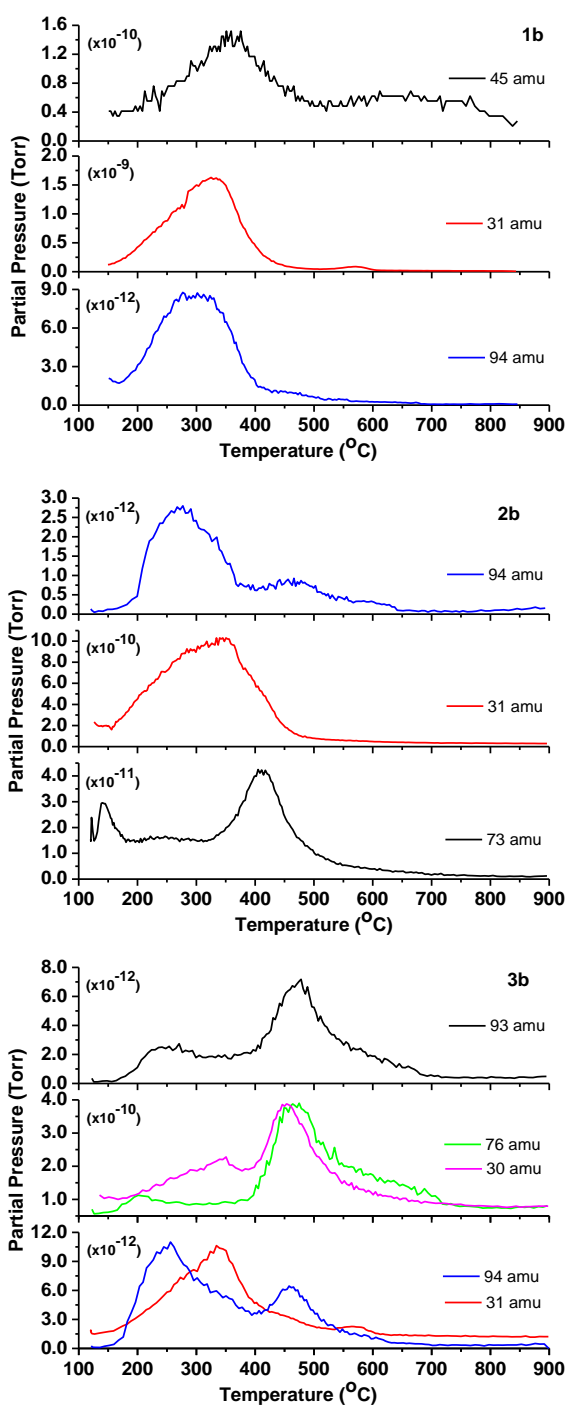


Figure 3. Mass trace of ethoxy (45 amu), methoxy (31 amu) and methylpyridinium (94 amu) fragment given off during the heating of **1b**; Mass trace of methylpyridinium (94 amu), methoxy (31 amu) and ethyl formyl (73 amu) fragment given off during the heating of **2b**; Mass trace of phenoxy (93 amu), (green) phenyl (76 amu), (magenta) nitroso (30 amu), (red) methoxy (31 amu) and (blue) methylpyridinium (94 amu) fragment given off during the heating of **3b**. Data were recorded in flowing He (20 mL min^{-1}) at a ramp rate of $10 \text{ }^\circ\text{C min}^{-1}$ to $900 \text{ }^\circ\text{C}$ after being held at $120 \text{ }^\circ\text{C}$ for 30 mins to remove any residual solvent.

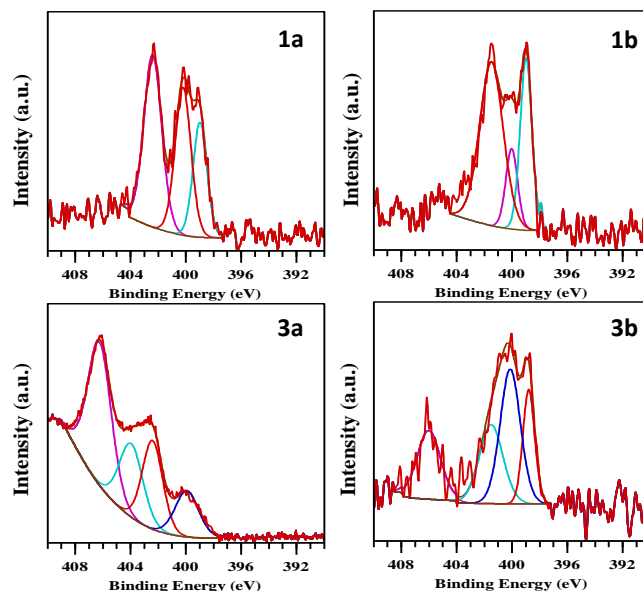


Figure 4. Deconvoluted N 1s XPS spectra of the pyridinium salt modified SWCNTs (**1a** and **3a**) and indolizine modified SWCNTs (**1b** and **3b**). The data were fitted using a Tougaard background. Peak positions were constrained to $\pm 0.2 \text{ eV}$ and were fitted using a GL(30) lineshape. Peak FWHM was also constrained in the region 1-3.

Fluorescence properties of indolizine modified light-emitting SWCNTs. The presence of fluorescent groups, so-called indolizine heterocycles, on nanotube surface was also confirmed by fluorescence spectroscopy where the studies showed that the indolizine functionalized SWCNTs (**1b** and **2b**) emitted light upon excitation (Figure 5). Excitation of **1b** and **2b** at 330 nm resulted in a blue emission at *ca.* 404 nm . To compare, free indolizine (**FI**), 3-ethyl 1,2-dimethyl indolizine-1,2,3-tricarboxylate was synthesised following the literature⁴⁵ via the addition of ethyl-2-bromoacetate to pyridine to afford *N*-(ethoxycarbonylmethyl)-pyridinium bromide which undergoes the 1,3-dipolar cycloaddition reaction with DMAD in the presence of a base (NET_3). (see *experimental section and ESI Scheme S1*) Compared to **1b** and **2b**, excitation of **FI** at 330 nm resulted in a blue shifted emission at *ca.* 382 nm , suggesting an electron transfer between electron rich indolizine and SWCNT upon the covalent attachment of indolizines to SWCNT surface. Control experiments mechanically mixing the FI with purified SWCNTs followed by washing with THF, acetone and ethanol showed no sign of fluorescence indicating that the fluorescence is not due to the physically adsorbed fluorescent indolizines (Figure 5). In contrast to **1b** and **2b**, excitation of **3b** at 330 nm showed no sign of fluorescence (Figure 5). It was no surprise since the structures like **3b** bearing strong electron withdrawing groups (*e.g.* $-\text{NO}_2$ groups) are likely to be quenched.⁵¹ Nitro groups of **3b** were reduced to amine ($-\text{NH}_2$) moieties using Sn/HCl ⁵² to synthesize amino group modified SWCNTs (**3c**) (Scheme 1). As expected, excitation of **3c** at 330 nm emitted at 430 nm following the conversion (Figure 5). XPS was used to confirm the reduction of nitro (NO_2) groups into amines (NH_2). N 1s XPS spectrum of **3c** showed three components positioned at 406.4 , 401.0 and 399.2 eV , corresponding to nitro groups ($-\text{NO}_2$),²³ the indolizine ring nitrogen ($-\text{N}<$)⁴⁹ and pyridinic nitrogen,³⁵ respectively (see *ESI Figure S2*). Decrease in the ratio of the relative peak intensity between the peak positioned at *ca.* 406.4 eV (nitro group nitrogen) and $\sim 400 \text{ eV}$ (pyridinic nitrogen) ($I_{406}/I_{400} = 0.57$) in N 1s XPS spectrum of **3b** (see *Figure 4*)

suggested that nitro groups were almost reduced when compared to the N 1s XPS spectrum of **3c** with I_{406}/I_{400} ratio of 0.08 (see *ESI Figure S2*).

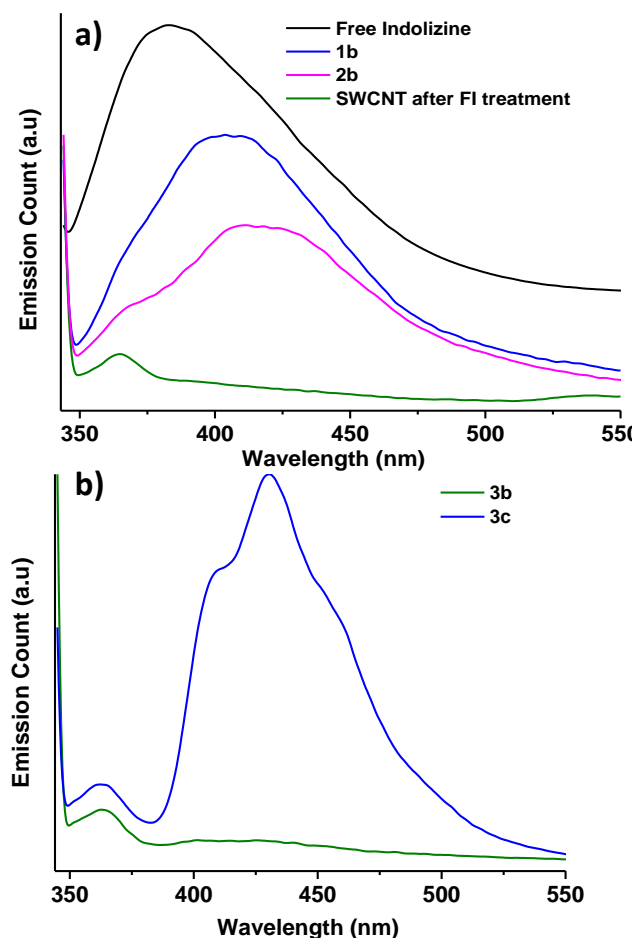


Figure 5. Normalized and offset fluorescence spectra of a) synthesized free indolizine (**FI**) structure (black line), **1b** (blue line), **2b** (magenta line), the control experiment of mechanically mixing purified SWCNTs with FI (olive line) recorded in CH_3CN ; b) **3b** (olive line) and **3c** (blue line) recorded in CH_3CN . Curves in Figure 6a and 6b are in top-down and down-top order, respectively.

Furthermore, the presence of a significant tail in the green region (~ 500 nm) of the emission spectra allowed us to optically image modified SWCNT materials (**1b**, **2b** and **3c**). **Figure 6** shows the white light optical image (left) and the epi-fluorescence image (right) of indolizine modified SWCNTs (**1b**, **2b** and **3c**). Fluorescence images were recorded using excitation light transmitted through a 420 to 480 nm excitation filter and fluorescence observed after passage through a 500 nm emission filter (Olympus CX-DMB-2 cube). The green spots can be clearly seen on the epi-fluorescence image (right) of modified SWCNTs (**1b**, **2b** and **3c**) as an indication of covalently attached light emitting indolizine groups on SWCNT surface, suggesting that the quantum efficiency of the emitted light is probably sufficient for practical applications (e.g. fluorescent imaging) (**Figure 6**). However, we were unable to calculate the absolute quantum efficiencies of the indolizine modified SWCNTs (**1b**, **2b** and **3c**) due to the strong scattering and absorption of the SWCNTs. As comparison it was possible to determine the quantum

yield of the **FI** heterocycle. The fluorescence quantum yield (Φ_f) of **FI** was determined from the corrected fluorescence spectra as 0.055, using anthracene dissolved in ethanol as a standard ($\Phi_f^{\text{st}} = 0.27$ at 25 °C).⁵¹

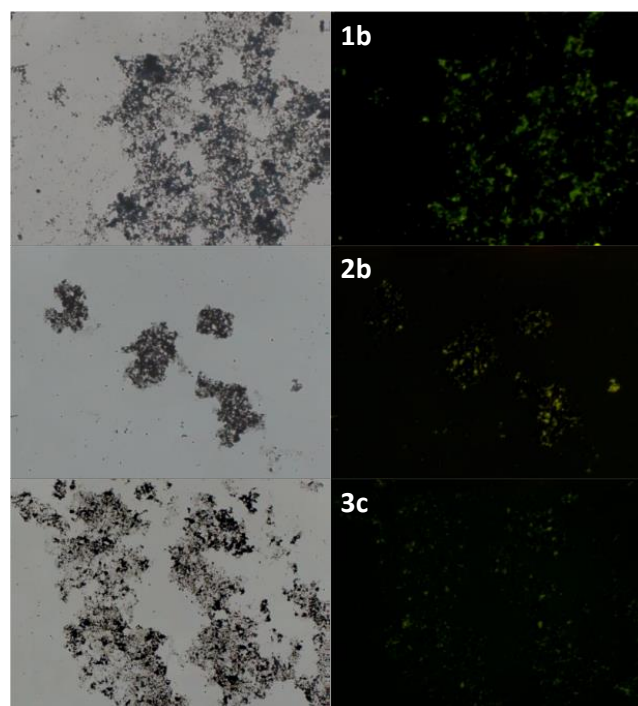


Figure 6. Unmodified white light transmission image (left) and fluorescence image (right) of indolizine functionalized SWCNTs (**1b**, **2b** and **3c**) taken using an Olympus CX41 optical microscope, field of view 718 x 533 μm .

Solution state photochemical sensing properties of indolizine modified light-emitting SWCNTs. With the given fluorescent properties it is expected that indolizine modified SWCNTs may be used as molecular sensing probes. Indolizine modified light-emitting SWCNTs (**1b**) was used as a *host molecule* to probe potentially dangerous nitroaromatics photochemically in solution-state. Phenol (**P**), 2-nitrophenol (**2NP**), 3-nitrophenol (**3NP**), 4-nitrophenol (**4NP**), 4-nitrotoluene (**4NT**) and 2,4-dinitrotoluene (**2_4NT**) were selected as guest molecules. A literature method has been followed to evaluate the solution phase photochemical sensing properties of **1b**.⁵³ Shortly, a stock solution of **1b** (~ 1.50 $\mu\text{g}/\text{mL}$, $\sim 1.25 \times 10^{-4}$ mol/L) and the guest molecules (1×10^{-4} mol/L) were prepared in acetonitrile (CH_3CN) for fluorescence spectral analysis. Each time a 3 mL solution of **1b** was filled in a quartz cell of 1cm optical path length, and stock solutions of guest molecules were added into quartz cell portion wise (2, 2, 2, 2, 5, 5, 5, 25, 25, 25, 100 μL) and mixed for 10 seconds. Measurements were performed immediately after mixing. An excitation wavelength of 330 nm and a temperature of 25 °C were employed in all experiments. Emission spectra of the guest molecules in CH_3CN showed no emission upon excitation at 330 nm (see *ESI Figure S3*). Fluorescence response of **1b** (3 mL, $\sim 1.25 \times 10^{-4}$ mol/L) to the guest molecules was initially tested by adding known amount of aromatic compound (**P**, **2NP**, **3NP**, **4NP**, **4NT** and **2_4NT**) (200 μL , 1×10^{-4} mol/L). Aromatic nitrophenol derivatives (**2NP**, **3NP** and **4NP**) caused a significant decrease in the fluorescence intensity of **1b** compared to **P** and nitrotoluene derivatives (**4NT** and **2_4NT**). (see *ESI Figure S4*) Fluorescence spectra of **1b** after the guest molecule addition suggested that fluorescent quenching efficiency (FQE) of **4NP** was the highest

among the guest molecules although it was not the least electron deficient one. FQE was observed in the order of 4NP>2NP>3NP>P>4NT>2,4NT. (see ESI Figure S4). As expected, portion wise addition of 4NP (2, 2, 2, 2, 5, 5, 5, 25, 25, 25, 100 μL) showed a significant, regular decrease trend in fluorescence intensity of **1b**, suggesting an intermolecular interaction between **1b** and 4NP (Figure 7).

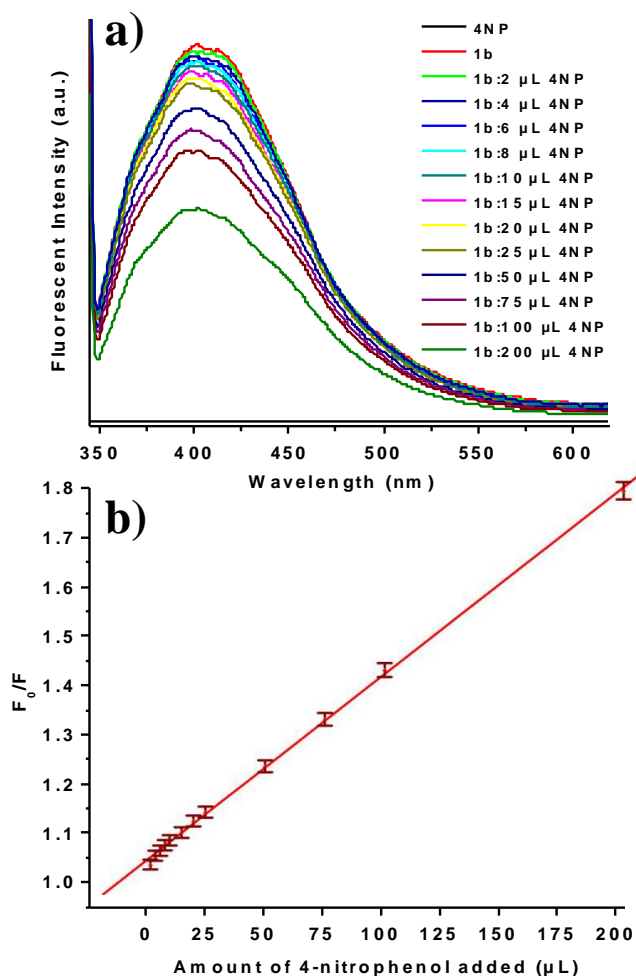


Figure 7. a) Change in the fluorescence spectra of **1b** (1.25×10^{-4} M) excited at 330 nm after the addition of 2, 4, 6, 8, 10, 15, 20, 25, 50, 75, 100, 200 μL equivalent of 4NP (1×10^{-4} M) dissolved in CH_3CN ; b) Stern-Volmer plot of the emission data provided by the change in fluorescence intensity after each 4NP addition.

Detection limit of photochemical sensing was estimated as 6.66×10^{-8} mol/L, considering the final concentration of 4NP after 2 μL addition. However, the detection limit may be lower than the estimated value since some of 4NP molecules are likely to be physically adsorbed by SWCNT surface and reduce the concentration of free 4NP in analysed solution. Adsorption of 4NPs was previously shown where a SWCNT based device was developed assembling nanotubes to electrodes using AC dielectrophoresis technique which allows the real-time detection of adsorbed nitrophenols in aqueous solution.⁵⁴ The Stern-Volmer relationship allows us to investigate the kinetics of a photophysical intermolecular deactivation process and, luminescence in solution

obeys the linear Stern-Volmer relationship,⁵⁵ $F_0/F = 1 + k_q\tau_0 \cdot [Q]$, where F_0 denotes the initial intensity of the fluorescent species without quencher, F represents the final intensity of the fluorescent species with quencher, k_q is the quencher rate coefficient, τ_0 is the fluorescence lifetime of the fluorescent species without a quencher and $[Q]$ is the concentration of the quencher. The Stern-Volmer plot constructed by the emission data obtained from the addition of 4NP to **1b** displayed a linear profile, probably indicating a single set of fluorophores, all equally accessible to the quencher (Figure 8).⁵⁶ Similarly, fluorescent quenching of **1b** using other guest molecules (P, 2NP, 3NP, 4NT and 2,4NT) was also studied. Addition of 2NP and 3NP displayed similar decreasing trend in fluorescent intensity of **1b** while the change in the fluorescent intensity upon the addition of P, 4NT and 2,4NT is not significant. (see ESI Figure S5-S9).

In order to further explore the intermolecular interactions between **1b** and 4NP, photochemical sensing properties of free indolizine (FI) structure, as a model, were also studied by fluorescence spectroscopy, FTIR and NMR. In agreement with **1b**, fluorescence spectral analysis of FI (3 mL, 2.09×10^{-7} M) in the presence of P, 2NP, 3NP, 4NP, 4NT and 2,4NT (200 μL , 1×10^{-4} mol/L) showed similar decreasing trend in the fluorescent intensity of FI, displaying a FQE order of 4NP>2NP>3NP>P>4NT>2,4NT. (see ESI Figure S4) Given the highest ability of 4NP to quench the fluorescence of FI this process was further investigated performing binding experiments. Similar to **1b**, FI was titrated with 4NP. As expected, similar trend in the fluorescence intensity of FI was observed after the addition of 4NP, confirming that the change in intensity is purely due to the intermolecular interactions between host and guest molecules. (see ESI Figure S10) It further confirmed that SWCNTs were functionalized by light-emitting indolizine groups that are able to sense particularly nitrophenol derivatives.

To investigate the nature of intermolecular interactions between FI and 4NP, spectroscopic analysis of the FI, 4NP and possible FI:4NP complex were carried out by NMR and FTIR. Equimolar amounts of vacuum-dried FI (10.64 mg, 3.28×10^{-2} mmol) and 4NP (4.5 mg, 3.28×10^{-2} mmol) were dissolved in 1 mL of anhydrous freeze-dried CDCl_3 for NMR spectroscopy analysis. Dry experimental conditions ensured that there was no possible proton exchange with water. Figure S11 shows the ^1H NMR spectra of FI, 4NP and the mixture (FI:4NP). The ^1H NMR spectrum of FI:4NP showed that the hydroxyl proton of 4NP (H_a) at 5.74 ppm disappeared upon mixing with FI, suggesting a strong intermolecular interaction that can probably be attributed to H-bonding interaction/proton transfer between hydroxyl proton of 4NP and FI.^{43, 57, 58} However, no significant signal shift was observed for the aromatic protons H_c , H_e , H_j and H_k , probably indicating weak or no π - π interactions between FI and 4NP. Complementary FTIR spectroscopy further confirmed the possible H-bonding interaction between FI and 4NP. FTIR spectra of compounds were recorded by dropping the stock solutions of the compounds (FI and 4NP) and the mixture (FI:4NP) on vacuum dried KBr disk. (see ESI Figure S12) FTIR spectrum of FI displayed three $\nu_{\text{C=O}}$ stretching vibrations at 1740, 1710 and 1695 cm^{-1} due to the presence of ethoxy and methoxy ester carbonyl groups. In contrast, FTIR spectrum of the mixture (FI:4NP) showed a strong broad $\nu_{\text{C=O}}$ stretching at 1700 cm^{-1} . Significant change in shape and position of the $\nu_{\text{C=O}}$ stretching bands of FI after the addition of 4NP revealed a strong intermolecular interaction, probably H-bonding between ester carbonyl of FI and hydroxyl proton of 4NP.^{43, 53, 59}

Solid state photochemical sensing properties of indolizine modified light-emitting SWCNTs. Due to their exceptional physical and chemical properties, SWCNTs can be used as solid

support materials for various applications including sensors.^{60, 61} Previously, it was shown that calculated photoluminescence quantum yield (PLQY) of fluorescent systems could be used as a tool to probe the sensing properties of fluorescent materials.⁶² Similar to previous work, solid state photophysical properties of **1b** and **3c** were studied by exposing them to saturated **4NP** vapour using a commercial spectrometer coupled with an integrating sphere.⁶² The vapour pressure of **4NP** at room temperature was previously reported as 1.9×10^{-5} mm Hg that corresponds to a vapour concentration of 19 ppb.⁶³ Fluorimetry experiments were performed on a quartz substrate coated with light-emitting SWCNTs. An excitation wavelength of 340 nm was selected for all measurements. PLQY of **1b** and **3c** was determined using the formalism outlined by de Mello where Φ_{PL} is PLQY, $E_i(\lambda)$ and $E_0(\lambda)$ are, respectively, the integrated luminescence as a result of direct excitation of SWCNTs and secondary excitation, $L_i(\lambda)$ and $L_0(\lambda)$ are the integrated excitation when SWCNTs are directly excited and the excitation light first hits the sphere wall, respectively and, $L_e(\lambda)$ is the integrated excitation profile for an empty sphere.⁶⁴

$$\phi_{\text{PL}} = \frac{E_i(\lambda) - (1-A)E_0(\lambda)}{L_e(\lambda)A} \quad A = \frac{L_0(\lambda) - L_i(\lambda)}{L_0(\lambda)}$$

Using the equation, PLQY of **1b** and **3c** was calculated as 0.9 and 0.3 %, respectively (Figure 8). As expected the PLQY of the modified SWCNTs was less than the free indolizines (**FI** and **FI_{NH2}**) with calculated PLQY of 5.5 and 3.5 %, respectively, probably due to the charge transfer from the electron rich indolizine system to the electron poor SWCNTs. These findings were in agreement with the blue-shift in emission spectra of **1b** and **3c** compared to pure spectra of **FI** and **FI_{NH2}**.⁴³ Similar decreasing trend in PLQY due to interaction between surface groups and SWCNT walls was previously reported in which the emission quantum yield of 2,4,6-triphenylpyrylium functionalized SWCNTs ($\Phi = 1\%$) was lower than 2,4,6-triphenylpyrylium alone ($\Phi = 33\%$).⁶⁵

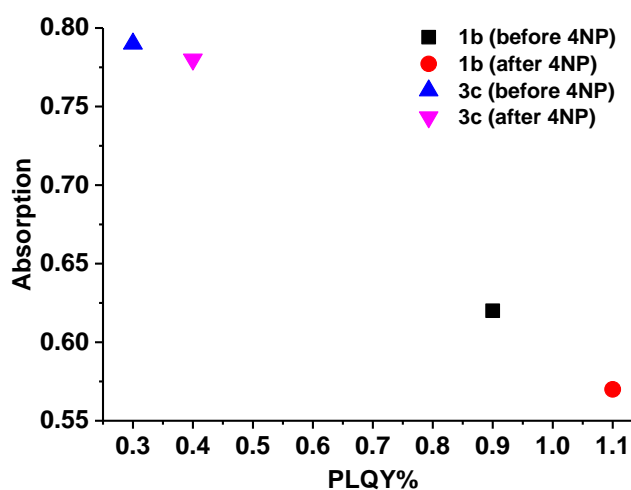


Figure 8. Calculated photoluminescence quantum yield of **1b** and **3c** versus absorption of **1b** and **3c** before/after exposing them to **4NP** vapour at room temperature.

The change in absorption (A in the equation) of the corresponding indolizine modified SWCNTs (**1b** and **3c**) can be used as a measure of the photochemical response to **4NP** vapour since the absorption of

fluorescent material is expected to change upon the adsorption of **4NP** to modified SWCNT surface.⁶² Before exposing to **4NP** vapour, the absorption values of **1b** and **3c** were determined as 0.62 and 0.79, respectively. The values decreased to 0.57 and 0.78 after exposing fluorescent SWCNTs to **4NP** vapour for 10 seconds (Figure 8). Furthermore, the calculated PLQY of **1b** and **3c** slightly increased to 1.1 and 0.4 %, respectively following **4NP** exposure (Figure 8). The change in absorption (A in the equation) of the corresponding indolizine modified SWCNTs (**1b** and **3c**) together with the change in the calculated PLQYs revealed that nitrophenol derivatives can be photochemically probed by indolizine modified light-emitting SWCNTs in solid-state at room temperature on a solid substrate.

Conclusions. A low temperature, highly controllable and efficient synthetic protocol to prepare indolizine modified light-emitting SWCNTs from pyridinium ylides generated on SWCNT surface was presented. Reactivity of the pyridine nitrogen lone pairs allowed the preparation of several quaternary pyridinium salt modified SWCNTs, which were subsequently used to synthesize pyridinium ylide functionalized SWCNTs and indolizine functionalized SWCNTs via 'click' chemistry. Shortly, the current study proposed a new perspective for the synthesis of carbon nanotube supported fluorescent molecules and their use in sensing of potentially dangerous nitrophenol derivatives. The indolizine modified light-emitting SWCNTs (**1b**, **2b** and **3c**) were shown to emit blue light (400–450 nm) upon excitation at ca. 330 nm. Fluorescent quenching of **1b** demonstrated that trace analysis of nitrophenol derivatives could be performed by indolizine modified light-emitting SWCNTs in both solution-state and solid-state. The fluorescent quenching was discussed work equally as well with **3c**. ¹H NMR and FTIR analysis of free indolizine (FI) structure suggested that the fluorescence of the modified materials quenched via probably an electron transfer from electron-rich indolizine to electron-deficient nitrophenolics through H-bonding interaction between ester carbonyls of indolizine and hydroxyls of nitrophenol. Optical microscopy images together with solid-state photophysical data revealed that indolizine modified fluorescent SWCNTs may potentially be used for imaging in cell transfection and drug delivery due to their high enough quantum efficiencies. Described methodology can be further expanded to introduce various molecules including cyclodextrins and cucurbituril with fluorescent indolizine tags on SWCNT surface that may be used for protein sensing and crystallisation. Furthermore the preparation of fluorescent hierarchical networks of carbon nanomaterials (e.g. carbon nanotubes and graphene) are anticipated via the reaction of bisdipolarophiles (e.g. bisacetylenes) with pyridinium ylides generated on carbon materials. The principles outlined here are expected to be applicable to other low dimensional materials including graphene and related inorganic layered materials.

Acknowledgements

The authors would like to thank EPSRC EP/G007314/1 for the funding of this project. M.K.B. thanks the Scientific and Technological Research Council of Turkey (TÜBİTAK).

Notes and references

^aDepartment of Chemistry, Durham University, South Road, Durham DH1 3LE, UK.

^bCurrent Address: Department of Chemical Engineering, University College London, London WC1E 7JE, UK

Electronic Supplementary Information (ESI) available: Normalized (at 330 nm) UV/vis-NIR spectra, recorded in *N,N*-dimethylformamide, of

purified SWCNTs and SWCNT-Py (Figure S1). Schematic representation of the synthesis of 3-ethyl 1,2-dimethyl indolizine-1,2,3-tricarboxylate (Free Indolizine) (Scheme S1). Devolved N 1s XPS spectrum of **3c** (Figure S3). Fluorescent spectra of 1b, P, 2NP, 3NP, 4NP, 4NT and 2_4NT in CH₃CN (Figure S4). Percentage decrease in fluorescence intensity of 1b and FI upon the addition of P, 2NP, 3NP, 4NP, 4NT and 2_4NT (Figure S5). Fluorescence spectra of 1b in the presence of 2, 4, 6, 8, 10, 15, 20, 25, 50, 75, 100, 200 μL equivalent of P, 2NP, 3NP, 4NP and 2_4NT (Figure S6-S10). Fluorescence spectra of FI in the presence of 2, 4, 6, 8, 10, 15, 20, 25, 50, 75, 100, 200 μL equivalent of 4NP (Figure S11). ¹H NMR spectra of 4NP, FI and possible FI:4NP complex formed (Figure S12). FTIR spectra of FI, 4NP and possible FI:4NP complex formed (Figure S13). See DOI: 10.1039/b000000x/

1. M. R. Sambrook and S. Notman, *Chemical Society Reviews*, 2013, **42**, 9251-9267.
2. M. D. Shirsat, T. Sarkar, J. Kakoullis, Jr., N. V. Myung, B. Konnanath, A. Spanias and A. Mulchandani, *Journal of Physical Chemistry C*, 2012, **116**, 3845-3850.
3. F. Wang, H. Gu and T. M. Swager, *Journal of the American Chemical Society*, 2008, **130**, 5392-+.
4. A. M. Muenzer, M. Heimgreiter, K. Melzer, A. Weise, B. Fabel, A. Abdellah, P. Lugli and G. Scarpa, *Journal of Materials Chemistry B*, 2013, **1**, 3797-3802.
5. J. Kong, N. R. Franklin, C. W. Zhou, M. G. Chapline, S. Peng, K. J. Cho and H. J. Dai, *Science*, 2000, **287**, 622-625.
6. P. G. Collins, K. Bradley, M. Ishigami and A. Zettl, *Science*, 2000, **287**, 1801-1804.
7. H. Jin, D. A. Heller, J.-H. Kim and M. S. Strano, *Nano Letters*, 2008, **8**, 4299-4304.
8. D. R. Kauffman, C. M. Shade, H. Uh, S. Petoud and A. Star, *Nature Chemistry*, 2009, **1**, 500-506.
9. S.-Y. Ju, W. P. Kopcha and F. Papadimitrakopoulos, *Science*, 2009, **323**, 1319-1323.
10. E. S. Jeng, J. D. Nelson, K. L. J. Prather and M. S. Strano, *Small*, 2010, **6**, 40-43.
11. J.-H. Kim, D. A. Heller, H. Jin, P. W. Barone, C. Song, J. Zhang, L. J. Trudel, G. N. Wogan, S. R. Tannenbaum and M. S. Strano, *Nature Chemistry*, 2009, **1**, 473-481.
12. M. J. O'Connell, S. M. Bachilo, C. B. Huffman, V. C. Moore, M. S. Strano, E. H. Haroz, K. L. Rialon, P. J. Boul, W. H. Noon, C. Kittrell, J. P. Ma, R. H. Hauge, R. B. Weisman and R. E. Smalley, *Science*, 2002, **297**, 593-596.
13. P. W. Barone, S. Baik, D. A. Heller and M. S. Strano, *Nature Materials*, 2005, **4**, 86-U16.
14. Y.-L. Zhao, L. Hu, G. Gruener and J. F. Stoddart, *Journal of the American Chemical Society*, 2008, **130**, 16996-17003.
15. Z. Dong, B. Yang, J. Jin, J. Li, H. Kang, X. Zhong, R. Li and J. Ma, *Nanoscale Research Letters*, 2009, **4**, 335-340.
16. Z. Dong, J. Jin, W. Zhao, H. Geng, P. Zhao, R. Li and J. Ma, *Applied Surface Science*, 2009, **255**, 9526-9530.
17. L. Zhang, L. Tao, B. Li, L. Jing and E. Wang, *Chemical Communications*, 2010, **46**, 1476-1478.
18. H. Hu, B. Zhao, M. A. Hamon, K. Kamaras, M. E. Itkis and R. C. Haddon, *Journal of the American Chemical Society*, 2003, **125**, 14893-14900.
19. B. K. Price and J. M. Tour, *Journal of the American Chemical Society*, 2006, **128**, 12899-12904.
20. M. S. Strano, *Journal of the American Chemical Society*, 2003, **125**, 16148-16153.
21. M. K. Bayazit and K. S. Coleman, *Journal of the American Chemical Society*, 2009, **131**, 10670-10676.
22. N. Tagmatarchis and M. Prato, *J. Mater. Chem.*, 2004, **14**, 437-439.
23. M. K. Bayazit, N. Celebi and K. S. Coleman, *Materials Chemistry and Physics*, 2014, **145**, 99-107.
24. M. K. Bayazit and K. S. Coleman, *Chemistry-an Asian Journal*, 2012, **7**, 2925-2930.
25. M. K. Bayazit and K. S. Coleman, *Journal of Materials Science*, 2014, **49**, 5190-5198.
26. M. K. Bayazit, A. Suri and K. S. Coleman, *Carbon*, 2010, **48**, 3412-3419.
27. B. R. Azamian, K. S. Coleman, J. J. Davis, N. Hanson and M. L. H. Green, *Chemical Communications*, 2002, 366-367.
28. K. S. Coleman, A. K. Chakraborty, S. R. Bailey, J. Sloan and M. Alexander, *Chem. Mat.*, 2007, **19**, 1076-1081.
29. S. A. Hodge, M. K. Bayazit, K. S. Coleman and M. S. P. Shaffer, *Chemical Society Reviews*, 2012, **41**, 4409-4429.
30. M. S. Strano, C. A. Dyke, M. L. Usrey, P. W. Barone, M. J. Allen, H. W. Shan, C. Kittrell, R. H. Hauge, J. M. Tour and R. E. Smalley, *Science*, 2003, **301**, 1519-1522.
31. J. J. Stephenson, J. L. Hudson, S. Azad and J. M. Tour, *Chem. Mat.*, 2006, **18**, 374-377.
32. J. L. Bahr and J. M. Tour, *Chem. Mat.*, 2001, **13**, 3823-+.
33. J. L. Bahr, J. P. Yang, D. V. Kosynkin, M. J. Bronikowski, R. E. Smalley and J. M. Tour, *Journal of the American Chemical Society*, 2001, **123**, 6536-6542.
34. C. A. Dyke, M. P. Stewart, F. Maya and J. M. Tour, *Synlett*, 2004, 155-160.
35. M. K. Bayazit, L. S. Clarke, K. S. Coleman and N. Clarke, *Journal of the American Chemical Society*, 2010, **132**, 15814-15819.
36. H. Nandivada, X. W. Jiang and J. Lahann, *Adv. Mater.*, 2007, **19**, 2197-2208.
37. H. M. Li, F. O. Cheng, A. M. Duft and A. Adronov, *Journal of the American Chemical Society*, 2005, **127**, 14518-14524.
38. Z. Guo, L. Liang, J. J. Liang, Y. F. Ma, X. Y. Yang, D. M. Ren, Y. S. Chen and J. Y. Zheng, *J. Nanopart. Res.*, 2008, **10**, 1077-1083.
39. S. Campidelli, B. Ballesteros, A. Filoramo, D. D. Diaz, G. de la Torre, T. Torres, G. M. A. Rahman, C. Ehli, D. Kiessling, F. Werner, V. Sgobba, D. M. Guldi, C. Cioffi, M. Prato and J. P. Bourgoin, *Journal of the American Chemical Society*, 2008, **130**, 11503-11509.
40. M. Becuwe, D. Landy, F. Delattre, F. Cazier and S. Fourmentin, *Sensors*, 2008, **8**, 3689-3705.
41. G. H. Yue, Y. D. Wan, S. J. Song, G. C. Yang and Z. X. Chen, *Bioorganic & Medicinal Chemistry Letters*, 2005, **15**, 453-458.
42. B. J. Landi, H. J. Ruf, J. J. Worman and R. P. Raffaele, *J. Phys. Chem. B*, 2004, **108**, 17089-17095.
43. M. K. Bayazit and K. S. Coleman, *Arkivoc*, 2014, **4**, 362-371.
44. A. V. Rotaru, I. D. Druta, T. Oeser and T. J. J. Muller, *Helvetica Chimica Acta*, 2005, **88**, 1798-1812.
45. C. A. Henrick, E. Ritchie and W. C. Taylor, *Aust. J. Chem.*, 1967, **20**, 2441-2453.
46. L. Cen, K. G. Neoh, Q. Cai and E. T. Kang, *Journal of Colloid and Interface Science*, 2006, **300**, 190-199.
47. J. T. Sampanthar, K. G. Neoh, S. W. Ng, E. T. Kang and K. L. Tan, *Adv. Mater.*, 2000, **12**, 1536-1539.
48. P. Actis, G. Caulliez, G. Shul, M. Opallo, M. Mermoux, B. Marcus, R. Boukherroub and S. Szunerits, *Langmuir*, 2008, **24**, 6327-6333.
49. C. Zhang, Z. G. Lai and F. C. Lu, *Polymer*, 1991, **32**, 3075-3079.
50. P. Brant and R. D. Feltham, *Journal of Organometallic Chemistry*, 1976, **120**, C53-C57.
51. A. Vlahovici, I. Druta, M. Andrei, M. Cotlet and R. Dinica, *Journal of Luminescence*, 1999, **82**, 155-162.
52. F. D. Bellamy and K. Ou, *Tetrahedron Letters*, 1984, **25**, 839-842.
53. N. She, M. Gao, L. Cao, A. Wu and L. Isaacs, *Organic Letters*, 2009, **11**, 2603-2606.
54. N. Liu, X. Cai, Q. Zhang, Y. Lei and M. B. Chan-Park, *Electroanalysis*, 2008, **20**, 558-562.
55. H. T. Yu, W. J. Colucci, M. L. McLaughlin and M. D. Barkley, *Journal of the American Chemical Society*, 1992, **114**, 8449-8454.
56. J. R. Lakowicz, *Principles of Fluorescence Spectroscopy*, 3rd Edition edn., Springer, Newyork, 2006.
57. J. P. M. Lommerse, S. L. Price and R. Taylor, *Journal of Computational Chemistry*, 1997, **18**, 757-774.

Journal Name

58. P. K. Dasgupta, S. P. Moulik and A. R. Das, *Bulletin of the Chemical Society of Japan*, 1991, **64**, 3156-3159.
59. K. Dharmalingam, K. Ramachandran and P. Sivagurunathan, *Spectrochimica Acta Part a-Molecular and Biomolecular Spectroscopy*, 2007, **66**, 48-51.
60. J. J. Davis, K. S. Coleman, B. R. Azamian, C. B. Bagshaw and M. L. H. Green, *Chemistry-a European Journal*, 2003, **9**, 3732-3739.
61. W. Feng, W. Luo and Y. Feng, *Nanoscale*, 2012, **4**, 6118-6134.
62. L. O. Palsson and A. P. Monkman, *Adv. Mater.*, 2002, **14**, 757-758.
63. M. K. K. Oo, Y. Guo, K. Reddy, J. Liu and X. Fan, *Analytical Chemistry*, 2012, **84**, 3376-3381.
64. J. C. deMello, H. F. Wittmann and R. H. Friend, *Adv. Mater.*, 1997, **9**, 230-&.
65. C. Aprile, R. Martin, M. Alvaro, H. Garcia and J. C. Scaiano, *Chem. Mat.*, 2009, **21**, 884-890.